Intrachain Exciton Dynamics in Conjugated Polymer Chains in Solution

Oliver Robert Tozer[1,2] and William Barford[1]

[1] *Department of Chemistry, Physical and Theoretical Chemistry Laboratory, University of Oxford, Oxford, OX1 3QZ, United Kingdom*

[2] *University College, University of Oxford, Oxford, OX1 4BH, United Kingdom*

Abstract

We investigate exciton dynamics on a polymer chain in solution induced by the Brownian rotational motion of the monomers. Poly(para-phenylene) is chosen as the model system and excitons are modeled via the Frenkel exciton Hamiltonian. The Brownian fluctuations of the torsional modes were modeled via the Langevin equation.

The rotation of monomers in polymer chains in solution has a number of important consequences for the excited state properties. First, the dihedral angles assume a thermal equilibrium which causes off-diagonal disorder in the Frenkel Hamiltonian. This disorder Anderson localizes the Frenkel exciton center-of-mass wavefunctions into super-localized local exciton ground states (or LEGSs) and higher-energy more delocalized quasi extended exciton states (QEESs). LEGSs correspond to chromophores on polymer chains. The second consequence of rotations – that are low-frequency – is that their coupling to the exciton wavefunction causes local planarization and the formation of an exciton-polaron. This torsional relaxation causes additional self-localization. Finally, and crucially, the torsional dynamics cause the Frenkel Hamiltonian to be time-dependent, leading to exciton dynamics. We identify two distinct types of dynamics.

At low temperatures the torsional fluctuations act as a perturbation on the polaronic nature of the exciton state. Thus, the exciton dynamics at low temperatures is a small-displacement diffusive adiabatic motion of the exciton-polaron as a whole. The temperature dependence of the diffusion constant has a linear dependence, indicating an activationless process. As the temperature increases, however, the diffusion constant increases at a faster than linear rate, indicating a second non-adiabatic dynamics mechanism begins to dominate. Excitons are thermally activated into higher energy more delocalized exciton states (i.e., LEGSs and QEESs). These states are not self-localized by local torsional planarization. During the exciton's temporary occupation of a LEGS – and particularly a quasi-band QEES – its motion is semi-ballistic with a large group velocity. After a short period of rapid transport, the exciton wavefunction collapses again into an exciton-polaron state. We present a simple model for the activated dynamics which is in agreement with the data.

I. INTRODUCTION

In solution conjugated polymers tend to be rather flexible as a result of the torsional motion of their monomer units. These torsional degrees of freedom have relatively low frequencies and shallow potentials, allowing for significant rotations of the molecular units away from their equilibrium geometries at finite temperatures. This means that even at temperatures approaching absolute zero there will be some level of disorder present in conjugated polymers, which is one of the major factors affecting the structure and characteristics of their excited electronic states. For example, the absorption and emission spectra of polymers, as well as their energy and charge transport properties, are significantly affected by the Anderson localization of the states that arises from the torsional disorder.[1,2] Thus, a significant amount of work is currently being put into investigating the nature of charge[3–7] and exciton transport[8,9] in disordered linear chains.

In this work we focus on modeling the torsional dynamics of a poly(para-phenylene) (PPP) chain in solution in order to determine the dynamics of Frenkel excitons in conjugated polymers as a consequence of the rotation of the monomer units. The migration distance (i.e., the expectation value of the distance an exciton travels before radiatively decaying) is an important quantity as in organic electronic devices the exciton needs to be able to move far enough to reach a heterojunction while avoiding non-radiative traps. Although in the solid state the torsional motion will be suppressed by steric effects, the solvated PPP chain investigated in this paper is used as a model to investigate the potential mechanisms of intrachain exciton transport in these systems without the added complication of interchain effects.

The model that has been used throughout this work treats the rotational motion of the phenylene rings using a Langevin dynamics algorithm,[6,9,10] where the solution surrounding the polymer chain is assumed to impart energy into the torsional modes via Brownian random impulses that are neither spatially nor temporally correlated.[11,12]. Thus, the fluctuation-dissipation theorem is invoked to relate the friction from the solution to the thermal impulses the solution provides.[13] These torsional fluctuations cause the polymer chain to be a disordered system, resulting in Anderson localization of the exciton states on the chain.[2] The consequence of this localization is that the low energy exciton states form a series of highly localized, non-overlapping, essentially nodeless local exciton ground states

(LEGSs),[14,15] with the higher lying states being more delocalized quasi-extended exciton states (QEESs).

In addition to the Anderson localization of the vertical exciton states, the exciton states are further self-localized as they dynamically relax into exciton-polarons as planarization of the polymer torsional modes in the region of the exciton causes a relaxation of the excited electronic state. This polaron formation is treated rigorously by calculating the bond-order torque that is imparted by the exciton. We do not model self-localization via bond distortion because, as reported elsewhere, the high frequency C-C bond vibrations are not expected to cause exciton-polarons[16].

The Brownian forces on the polymer monomers that cause spatial and temporal torsional fluctuations have two consequences. First, as already noted, the instantaneous spatial fluctuations Anderson localize the Frenkel center-of-mass wavefunction. (This breaking of translational symmetry determines the positions of the self-localized exciton-polarons.) Second, the temporal fluctuations cause the exciton to migrate. (This process is sometimes referred to as Environmental Assisted Quantum Transport[17].) We identify two distinct transport processes.

First, at low temperatures there is small-displacement adiabatic motion of the exciton-polaron as a whole along the polymer chain, which might be characterized as 'crawling' motion. Second, at higher temperatures the torsional modes fluctuate enough to cause the exciton to be thermally excited out of the self-localized polaron state into a more delocalized LEGS or quasi-band QEES. While in this more delocalized state, the exciton momentarily exhibits quasi-band ballistic transport, before the wavefunction 'collapses' into an exciton-polaron in a different region of the polymer chain. We might characterize this large-scale displacement as non-adiabatic 'hopping' motion.

The role of exciton transport in disordered one-dimensional systems via higher-energy quasi-band states was discussed in ref[8], where in that work phonons in the condensed phase environment induced non-adiabatic transitions. Albu and Yaron used a similar model to ours to investigate excited state relaxation in polymers in solution[9].

In this work the motion of the exciton along the polymer chain is primarily modeled by projecting the instantaneous eigenstates of the Frenkel Hamiltonian[18] onto the exciton wavefunction from the previous timestep, and selecting the eigenstate with the largest overlap. We also investigate solutions of the time dependent Schrödinger equation for the Frenkel

exciton Hamiltonian coupled to the classical torsional modes (i.e., the Ehrenfest approximation for quantum-classical dynamics). We show that the two methods agree for the adiabatic dynamics, but the Ehrenfest dynamics fails to properly describe non-adiabatic dynamics, because of its well-known failure to properly describe relaxation processes[19].

In the following section the model and methodology, including the Langevin dynamics algorithm and the Frenkel exciton Hamiltonian, are discussed, while section III has further details about polaron formation on the PPP chains. Section IV presents data on the exciton diffusion rates in PPP, as well as detailing the proposed mechanisms for this migration in the low temperature regime and at higher temperatures. A brief summary of the conclusions made in this work is given in the final section.

II. MODEL AND METHODOLOGY

A. Frenkel Exciton Model

The poly(para-phenylene) (PPP) chains that are the focus of this work are modeled using the coarse-grained Frenkel exciton Hamiltonian. In this model, the polymer chain is formed of N sites, with each site representing one of the phenylene rings in the polymer chain. The Frenkel exciton Hamiltonian,[18] H_F, is then given by

$$H_F = \sum_{n=1}^{N} E_0 a_n^\dagger a_n + \sum_{n=1}^{N-1} J_{n,n+1}(a_n^\dagger a_{n+1} + a_{n+1}^\dagger a_n) \tag{1}$$

where E_0 is the monomer excitation energy of a Frenkel exciton, $a_n^\dagger$ (a_n) creates (destroys) a Frenkel exciton on monomer n of the PPP chain, and $J_{n,n+1} \equiv J_\nu$ is the Frenkel exciton hopping parameter across bond ν, which links monomers n and $(n+1)$. The exciton state vector, $|\Psi\rangle$, is then formed by a linear combination of single monomer Frenkel exciton basis states, $|n\rangle$, as

$$|\Psi\rangle = \sum_{n=1}^{N} \Psi_n |n\rangle \tag{2}$$

where Ψ_n is the exciton center-of-mass wavefunction.

The Frenkel exciton hopping parameter, J_ν, has two contributions.[15,20] The first of these is the through-space dipole-dipole component

$$J_{dd}^{mn} = \frac{\kappa_{mn}\mu_0^2}{4\pi\epsilon_r\epsilon_0 R_{mn}^3} \tag{3}$$

where μ_0 is the magnitude of the transition dipole moment on a single phenylene ring and R_{mn} is the distance between the centers of monomers m and n. κ_{mn} is an orientational factor given by

$$\kappa_{mn} = \mathbf{r_m} \cdot \mathbf{r_n} - \mathbf{3}(\mathbf{R_{mn}} \cdot \mathbf{r_m})(\mathbf{R_{mn}} \cdot \mathbf{r_n}) \tag{4}$$

where $\mathbf{R_{mn}}$ is a unit vector parallel to the vector joining the centres of phhenylene rings m and n, and $\mathbf{r_n}$ is a unit vector parallel to the transition dipole on ring n. Only the nearest-neighbour contributions to J_{dd} are considered in this work[21]. ($\kappa_{mn} = -2$ for collinear monomers.)

The second component of the Frenkel exciton hopping parameter is a through-bond, or superexchange, term which has been previously parameterized, and depends on the square of the cosine of the torsional angle, as the overlap of the π-orbitals on adjacent monomers is a significant factor in the magnitude of this term. As a result, disorder is introduced to the model as each of the monomers is assumed to have a torsional coordinate, ϕ_n, which is allowed to deviate from equilibrium. The dihedral angle across bond ν between monomers n and $(n+1)$, $\theta_\nu = (\phi_{n+1} - \phi_n)$. As has been discussed elsewhere,[15] the disorder in these angles has a significant effect on the eigenstates of the Frenkel Hamiltonian as the overall exciton hopping parameter is given by

$$J_\nu = J_{dd} + J_{se} \cos^2 \theta_\nu \tag{5}$$

where $J_{dd} = -0.4$ eV is the dipole-dipole and $J_{se} = -1.0$ eV is the super-exchange component of the exciton transfer integral.

In solution, the dihedral angle across bond ν is assumed to have an equilibrium value, θ^0_ν, of $\pm 40^\circ$ due to the steric interactions between adjacent monomers. In the absence of an exciton the torsional mode is assumed to behave harmonically, such that there is a restoring torque on phenylene ring n

$$\Gamma^{el}_n = -K(\delta\theta_{\nu-1} - \delta\theta_\nu), \tag{6}$$

where $\delta\theta_\nu = (\theta_\nu - \theta^0_\nu)$ is the deviation of the torsional angle, θ_ν, from the equilibrium torsional angle, θ^0_ν. The spring constant for the torsional modes of PPP, K, has a value of 1.13 eV. If a torsional mode is behaving harmonically, then there is a gaussian distribution of bond angles with a standard deviation given by[15]

$$\langle \sigma_\theta \rangle = \left(\frac{k_B T}{K} \right)^{\frac{1}{2}} \tag{7}$$

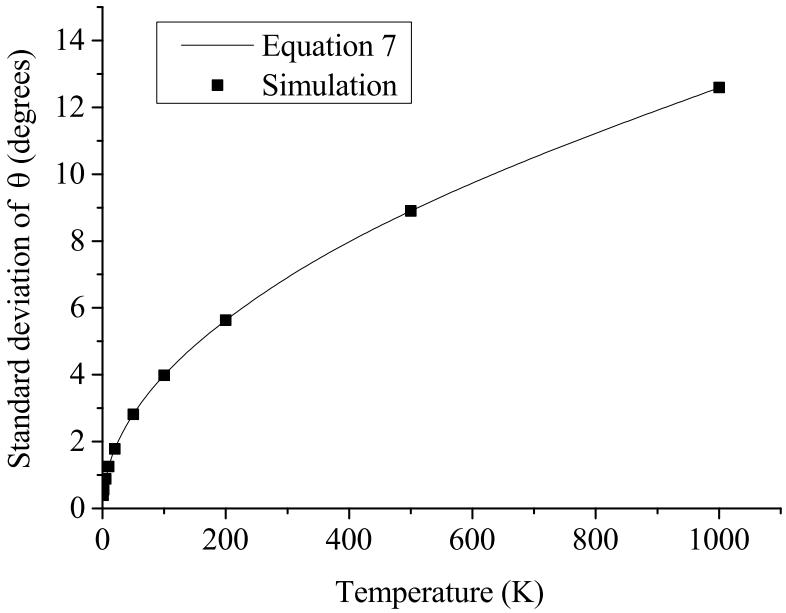

FIG. 1: The standard deviation of the torsional angles, θ_ν, of a poly(para-phenylene) chain in the absence of an exciton. The values are calculated after equilibration of a polymer chain containing 50000 phenylene rings.

where k_B is the Boltzmann constant and T is the temperature. The dynamics simulation used in this work (as described below) reproduces this distribution for a large range of temperatures, as shown in Fig. 1.

This disorder in the dihedral angles causes Anderson localization of the exciton center-of-mass wavefunctions, resulting in the low-energy exciton states being superlocalized into non-overlapping local exciton ground states (LEGSs),[14,15] which define the chromophores of a disordered conjugated polymer chain. As these states are essentially nodeless, they can be identified by calculating a signed value parameter, α, for each state, where[14]

$$\alpha = \left| \sum_{n=1}^{N} \Psi_n |\Psi_n| \right|. \tag{8}$$

A truly nodeless state will have a value of $\alpha = 1$, while a LEGS is generally defined as any state where $\alpha \geq 0.95$.

As each monomer of the PPP chain has the same chemical structure, we can assume that $E_0 = 0$ without loss of generality. Disorder could be introduced to this value in order to represent density fluctuations in the region of the monomers, resulting in variable local

dielectric constants. However, it is assumed that in solution this value will fluctuate rapidly, so taking the average value is justified.

In addition to the harmonic torque attempting to keep the torsional angles at their equilibrium value, there is a net torque on the phenylene rings due to the presence of an exciton, resulting in formation of an exciton-polaron. From the Hellmann-Feynman theorem, this torque is

$$\begin{aligned} \Gamma_n^{ex} &= -\left\langle \Psi \left| \frac{\partial H_F}{\partial \phi_n} \right| \Psi \right\rangle \\ &= -2J_{se}\Psi_n \left(\Psi_{n+1}\sin 2\theta_\nu - \Psi_{n-1}\sin 2\theta_{\nu-1}\right). \end{aligned} \tag{9}$$

The total systematic torque is

$$\Gamma_n^{syst} = \Gamma_n^{el} + \Gamma_n^{ex}. \tag{10}$$

B. Langevin Dynamics

In addition to the deterministic systematic torques (described above), there is a stochastic Brownian torque arising from the interactions between the solvent and the polymer. It is assumed that at each time step of the dynamics there will be an impulse on each phenylene ring of the polymer chain, causing it to rotate about its torsional axis. These torques are spatially uncorrelated, as it is assumed the phenylene rings are significantly larger than the solvent molecules. This means that any interaction between solvent and polymer will be local in nature. The stochastic torques are also temporally uncorrelated as the timestep of the simulation (10^{-14} s, unless otherwise stated) is significantly larger than the timescale of solvent interactions.

These assumptions are the basis of Langevin dynamics simulations, and the algorithm that has been used in this work closely follows that of van Gunsteren and Berendsen.[11] (This algorithm has been shown to be essentially equivalent to that of Allen.[12]) The equation of motion for phenylene ring n is given by

$$I\frac{d\Omega_n(t)}{dt} = -I\gamma\Omega_n(t) + \Gamma_n^{syst}(t) + R_n(t), \tag{11}$$

where $I = 9.119\times10^{-27}$ eVs^2 is the moment of inertia of a phenylene ring about its rotational axis, $\Omega_n = \frac{d\phi_n}{dt}$ is its angular velocity, and $R_n(t)$ is the stochastic torque on the ring due to the random fluctuations in the solvent. γ is the friction coefficient for the specific solvent and condition. In this work $\gamma = 10^{12}$ s^{-1}, unless otherwise stated.

The fluctuation-dissipation theorem states that the process by which kinetic energy in the system is converted into thermal energy of the surroundings can be directly related to the reverse process by which thermal energy is converted into kinetic energy. Specifically, the friction coefficient, γ, which determines the rate of dissipation of energy from the torsional modes, is also the parameter which determines the magnitude of the stochastic impulses by which energy is imparted on the phenylene rings by the solvent. By the fluctuation-dissipation theorem,[13] the distribution of random torques, $R_n(t)$, is given by

$$\langle R_n(0)R_m(t)\rangle = 2I\gamma k_B T\delta_{mn}\delta(t). \tag{12}$$

In addition to being both spatially and temporally uncorrelated, these torques are also assumed to be independent of the angular velocity of the phenylene ring and independent of the systematic torque, Γ_n^{syst}. These stochastic torques then form a gaussian distribution with a standard deviation of

$$\sigma_R = (2I\gamma k_B T)^{\frac{1}{2}}. \tag{13}$$

Although these impulses are uncorrelated with time, the same is not true for the torsional angles, as the angles at a given time will differ only slightly from the angles at an infinitesimaly earlier time. In order to characterize how long it takes for the PPP chain to equilibrate in the Langevin simulations, the auto-correlation function $\langle\delta\theta(t)\delta\theta(0)\rangle$ was calculated. By the definition of this variable, we expect the harmonic oscillations to decay with a time constant of γ, and the period of oscillations to depend on the frequency of the torsional modes. The autocorrelation function is plotted as a function of time for various parameters in Fig. 2, where it can be seen that the correlation function is well described by

$$\langle\delta\theta(t)\delta\theta(0)\rangle = \langle\delta\theta^2\rangle\cos(2\pi ft)\exp(-\gamma t) \tag{14}$$

where

$$\langle\delta\theta^2\rangle = \frac{k_B T}{K} \tag{15}$$

(in agreement with Eq. (7)) and f is the vibrational frequency of the torsional mode, which is 1.8×10^{12} s^{-1} for the PPP parameters used in this work.

For $\gamma = 10^{12}$ s^{-1} we see that the torsional motion is damped after several picoseconds. However, to be certain of equilibration in the dynamics an equilibration time (in the presence of an exciton) of at least 100 ps was used before each of the simulations in this work.

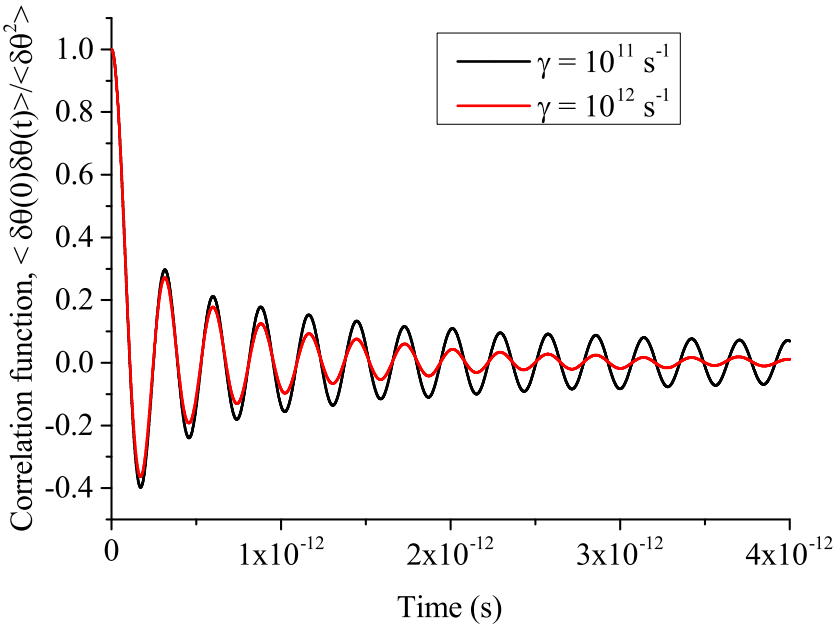

FIG. 2: The torsional angle auto-correlation function as a function of time for two values of frictional constant, γ. Changing the temperature has no effect on the time period or decay rate but affects the initial value of the autocorrelation function, $\langle \delta\theta^2 \rangle$, as shown in Eq. (15).

C. Exciton Wavefunction Dynamics

The Langevin dynamics algorithm is used to calculate a set of torsional angles at time $(t + \delta t)$ based on the angles and exciton wavefunction at the previous timestep. However, we still require a new exciton wavefunction as the exciton state at the previous timestep will no longer be a stationary state of the Hamiltonian as the dihedral angles will have changed. Previous work on this topic in the absence of a heat bath has calculated the new exciton state by numerically solving the time dependent Schrödinger equation (TDSE).[4] However, as described in Section IV C, the Ehrenfest approximation fails when coupled to a heat bath. Consqeuently, a time independent Schrödinger equation (TISE) method was used instead.

The TISE can be written as

$$H_F|\Phi\rangle = E|\Phi\rangle \tag{16}$$

and the TISE method used in this work involves finding the solutions of this equation by diagonalizing the Hamiltonian matrix of Eq. (1) at each timestep to find the Frenkel exciton eigenstates. Since the torsional degrees of freedom are much slower than the excitonic degrees

of freedom, we assume that the excitonic wavefunction evolves quasi-adiabatically. That is, its evolution is determined by calculating the instantaneous eigenstates of the Hamiltonian at time $(t + \delta t)$, i.e., $\{|\Phi(t + \delta t)\rangle\}$, and projecting them onto the target exciton eigenstate at the previous time step t, i.e., $|\Psi(t)\rangle$. The eigenstate with the largest overlap is selected to be the target exciton eigenstate at the next iteration, i.e., $|\Psi(t + \delta t)\rangle$.

Even though the exciton wavefunction is evolving infinitesimally slowly through a series of instantaneous eigenstates, this simulation does account for non-adiabatic transitions between bound exciton-polarons and delocalized quasi extended exciton states, as described in Section IV. Our results are, within statistical accuracy, independent of step sizes, Δt, for $\Delta t \leq 10^{-14}$ s.

D. Finite Chain Size

In numerical calculations there is always a possibility that the system size being considered is too small and finite size effects are influencing the results. As we are considering migration of an exciton over its entire lifetime, considering the entire system at all timesteps would require a model chain containing many thousands of monomer units to ensure there is negligible probability of the exciton reaching the chain end. However, as will be shown in the next section, the exciton localization length is significantly smaller than this value, suggesting methods to avoid such large chains.

In this work the exciton state under consideration was kept in the center of the chain at each timestep by removing monomers from one end of the chain and adding an equal number of monomers to the other end. The phenylene rings that are added are given a thermal distribution of torsional angles. In this way, the chain length can be significantly reduced as the only necessity is making sure that the exciton wavefunction fits comfortably on the chain. As the largest exciton sizes seen in the course of this work were just under 100 sites, a chain size of 200 monomers was used for all the calculations in this work. (We checked that our results are, within statistical accuracy, independent of chain sizes of more than 200 monomers.)

III. POLARON FORMATION

As can be seen from Eq. (1) and Eq. (5), the presence of an exciton will have an effect on the underlying nuclear geometry as a more planar structure has a larger exciton transfer integral, thus stabilizing the excitation. This means that in the absence of thermal fluctuations we might expect the nuclear geometry to planarize in the vicinity of the exciton, effectively digging a potential well which will trap and localize the exciton.[23] This expectation is correct if the normal modes to which the exciton couples are treated classically. However, if they are quantized the condition for self-localization is more complicated.

Self-localization[24] via coupling to harmonic modes occurs if the dressed particle becomes so heavy that its disorder-induced localization length is smaller than the intrinsic classical polaron size[16]. Since the localization length decreases as the particle's effective mass increases, and the effective mass increases as the frequency of the normal mode decreases[16,25], slower modes are more likely to self-localize polarons. As shown in ref[16], the high frequency C-C bond stretches (with an energy of ~ 0.2 eV) are too fast to localize polarons for reasonable values of disorder, while the low frequency torsional modes (with an energy of ~ 0.01 eV) are expected to localize polarons.

We therefore treat the torsional modes classically, and expect that in the low temperature limit the Langevin dynamics algorithm will result in the formation of a polaron that is virtually identical to the classical polaron calculated from a Hellmann-Feynman routine (i.e., setting the torque, $\Gamma_n = 0$ in Eq. (10)). The exciton densities for these two polarons, as well as that for an untrapped exciton, are shown in Fig. 3, where it can be seen that this is indeed the case. Figure 3 also shows that the deviation of the dihedral angles from equilibrium in the vicinity of the exciton-polaron at T = 0 K mirrors the exciton density.

At finite temperatures, where thermal fluctuations occur, we expect a combination of factors to affect the localization of the exciton. First, we still expect the exciton to attempt to form a polaron and be trapped in the potential well that is formed by these torsional distortions. However, it is possible that the thermally induced fluctuations in the torsional angles will affect the size of this exciton-polaron, as there is a non-negligible probability that the exciton will be excited out of its polaron potential well into a more delocalized state at high enough temperatures. Second, we expect the exciton states to be Anderson localized by the torsional disorder, even in the absence of coupling between the exciton and the nuclei.

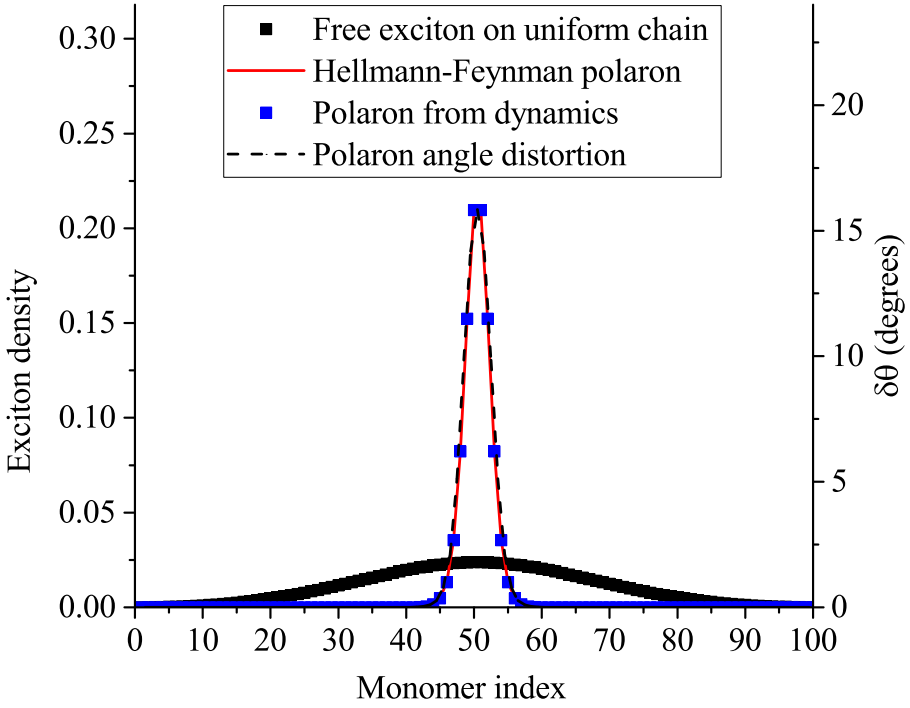

FIG. 3: The 'free' exciton density on a uniform chain (black squares) and the exciton density once equilibration has occurred in the Langevin dynamics at T = 0 K (blue squares). The classical polaron, as calculated by a Hellmann-Feynman calculation, is also plotted (red line) to show that the dynamics simulation accurately reproduces this result. Also shown is the deviation of the dihedral angles from equilibrium, $\delta\theta$, in the exciton-polaron state.

The size of the exciton center-of-mass wavefunction (or exciton localization length, ℓ) is calculated as[1]

$$\ell = 5.6\sqrt{\langle R^2\rangle - \langle R\rangle^2} \tag{17}$$

where

$$\langle R^l\rangle = \sum_{n=1}^{N} R^l |\Psi_n|^2 \tag{18}$$

and the factor of 5.6 arises from the ratio between the root-mean-square spread of a LEGS and the length of chain it occupies, as shown by Makhov and Barford.[1] The exciton localization length is a physically important value, as it can be directly related to the relative peak heights in the vibronic progression in both absorption and emission spectra of conjugated polymers[26,27] as well as potentially playing an important role in an explanation of other effects, such as ultrafast fluorescence depolarization[20,28,29] and exciton dynamics (as discussed

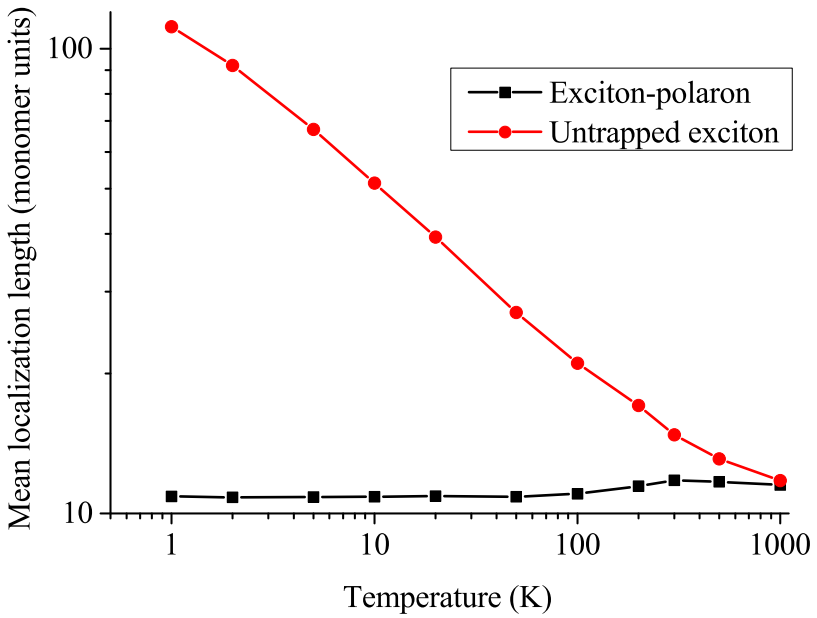

FIG. 4: The exciton localization length at various finite temperatures for the 'free' (i.e., 'untrapped') exciton (red circles) and exciton-polaron (i.e., 'self-trapped') (black squares). Although increasing the temperature causes a slight increase in the size of the exciton-polaron, this is only a very minor effect. As will be shown, this increase in size arises from the exciton escaping from the polaron potential well and being excited into a LEGS or QEES. The polaron binding energy is high enough for excitons in PPP that this is a rare occurrence even at high temperatures.

in Section IV B (see also refs[8,22]).

Figure 4 shows how the average localization length varies with temperature both with and without coupling between the exciton and the torsional modes (i.e., 'self-trapped' and 'free' exciton, respectively). The localization length for the 'free' exciton is determined by Anderson localization and follows $\ell \sim T^{-1/3}$. The localization length of the 'self-trapped' exciton slowly increases with temperature because of the thermal excitation of the exciton from the self-localized polaron to a more delocalized LEGS or QEES. The two values coincide when $k_B T$ equals the exciton-polaron binding energy, i.e., $T \sim 1500$ K.

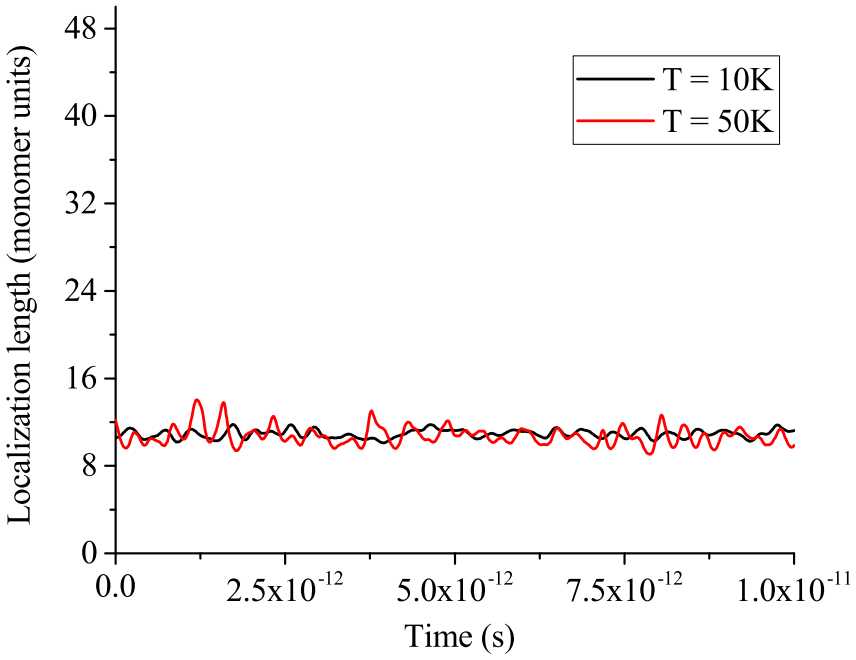

FIG. 5: The exciton localization length, given by Eq. (17), as a function of time for a single example trajectory at two low temperatures. The localization length remains virtually constant throughout, suggesting that the exciton remains self-localized in the polaron potential well at these temperatures.

IV. EXCITON MOTION

A. Low Temperature Exciton Dynamics

At low temperatures ($\lesssim$ 100 K) the exciton has only a small amount of thermal energy, and not nearly enough to regularly break free from its polaronic torsional distortions. The exciton binding energy at 0 K is 0.134 eV, which is equivalent to a temperature of over 1500 K. Thus, at low temperatures we expect the exciton-polaron to migrate adiabatically as a single unit. We expect this motion to be diffusive, as there is no preference for the exciton-polaron to migrate in either direction, and the timescales being observed are significantly longer than the timescales of the autocorrelation function of the torsional angles, meaning a random walk assumption is valid.

In order to verify that the exciton is in fact remaining in an exciton-polaron state, the

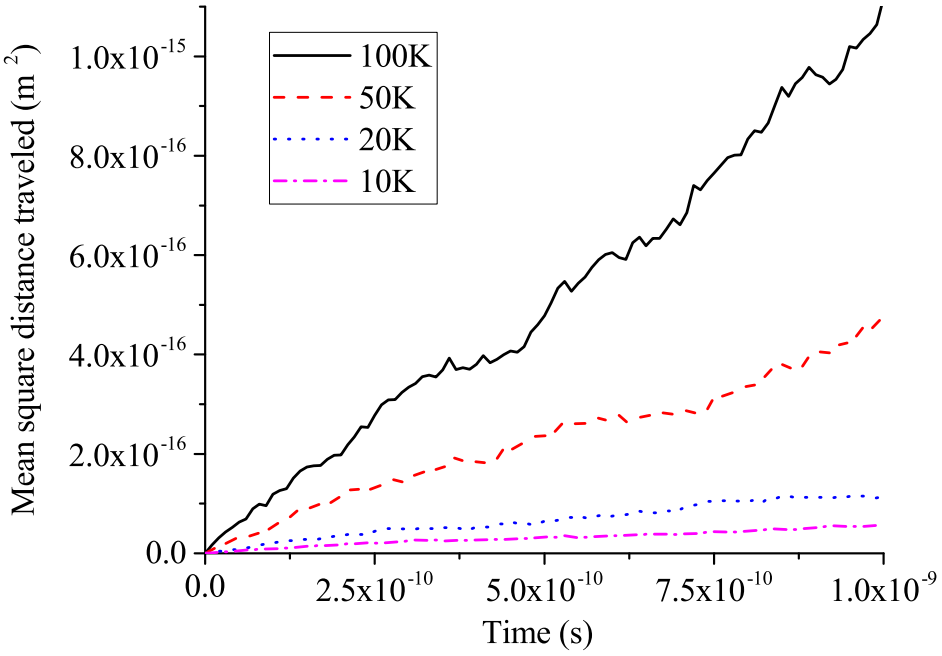

FIG. 6: The mean square distance traveled by an exciton at low temperatures. The motion is diffusive, as shown by the mean square distance, $\langle L^2 \rangle$, increasing linearly with time. Each line is an average of 150 trajectories, and $\gamma = 10^{12}$ s^{-1} throughout.

exciton localization length, defined in Eq. (17), is plotted as a function of time for a single trajectory of the exciton at two low temperatures in Fig. 5. It is apparent that the exciton localization length remains that of a self-localized exciton-polaron for the entire duration of the simulation, with no significant increases in size that would indicate that the exciton has been excited from a highly localized exciton-polaron into a more delocalized LEGS or QEES state. In addition, the signed-value parameter of Eq. (8) remained almost identical to 1 throughout, indicating that the exciton wavefunction remains nodeless at these low temperatures.

As a result of the random walk approximation that can be made, we expect the contour distance traveled by the particle center-of-mass to obey

$$\langle L^2 \rangle = 2D(T)t \tag{19}$$

where L is the distance traveled by the center-of-mass of the exciton, and $D(T)$ is the diffusion constant for the exciton centre-of-mass wavefunction at temperature T. Figure 6

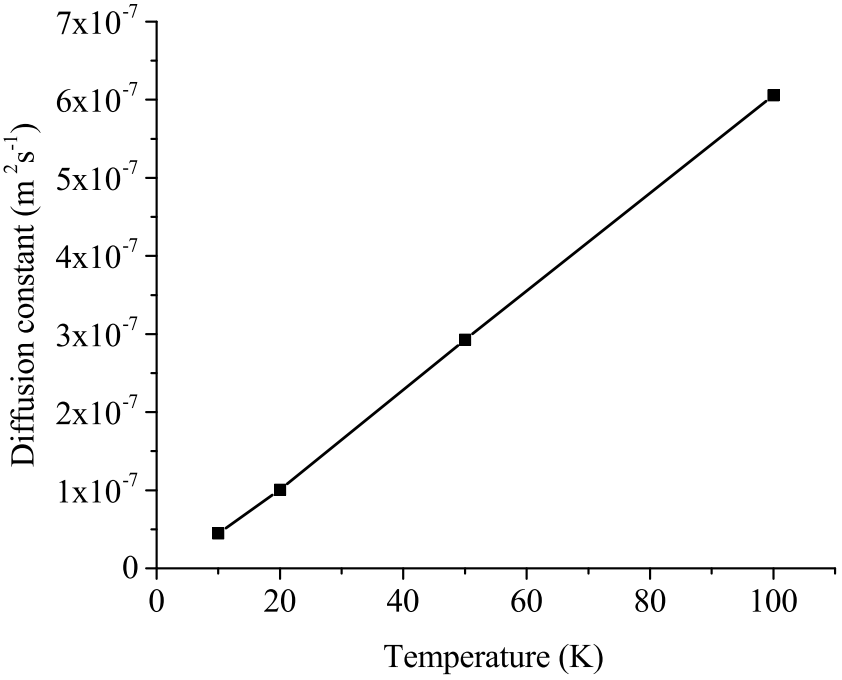

FIG. 7: The variation of the diffusion constant, D, of Eq. (19) as a function of temperature. In this low temperature regime, D appears to obey the Einstein-Smoluchowski relation given in Eq. (20).

shows how migration of the exciton occurs as a function of time for an ensemble average of trajectories at various low temperatures. It is apparent that the mean square distance traveled by the exciton does increase linearly with time, as predicted, and that a diffusion constant can therefore be extracted from the data.

This migration of the exciton-polaron in its entirity is likely to be an activationless process, as there is no barrier to the rotation of the phenylene rings from equilibrium, and any increase in elastic potential energy at one bond can be counteracted by a decrease in elastic potential energy at another, or by an increase in the stability of the exciton. As a result, we expect the exciton migration at low temperatures to obey the Einstein-Smoluchowski equation

$$D(T) = \mu k_B T \tag{20}$$

where μ is the mobility of the particle. The diffusion constants extracted from Fig. 6 are plotted as a function of temperature in Fig. 7, where we can see that there is a good linear relationship between them at low temperatures, implying that the random walk model is an

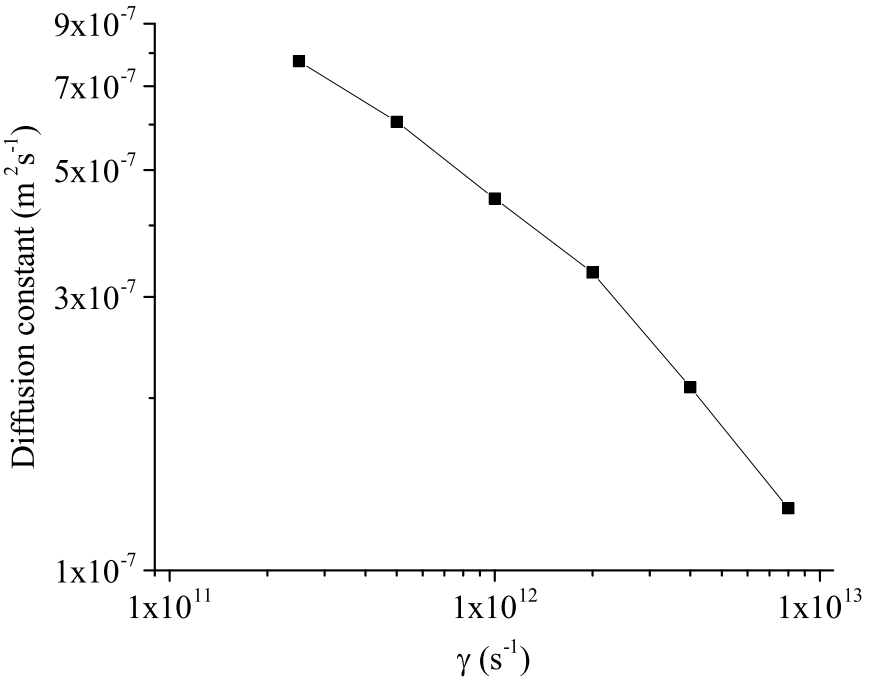

FIG. 8: The variation of the diffusion constant, D, of Eq. (19) as a function of γ, for an exciton migrating at a temperature of 50 K. Each diffusion constant is calculated from an ensemble average of 150 trajectories.

appropriate description for this low-temperature migration of excitons on PPP in solution.

In this low temperature regime, we also expect the friction coefficient of the torsional motion, γ, to have an effect on the diffusion of an exciton along the polymer chain, as this parameter has an effect on the rate of dissipation of the torsional motion and the magnitude of the impulses on the phenylene rings. The dependence of γ on the diffusion coefficient at 50 K is shown in Fig. 8, where it can be seen that increasing the value of the torsional frictional constant results in a decrease in the exciton diffusion constant. This γ dependence of the diffusion constant has a non-trivial functional form, and it suggests that in a more viscous solvent we would expect the exciton to migrate a shorter distance before radiatively decaying.

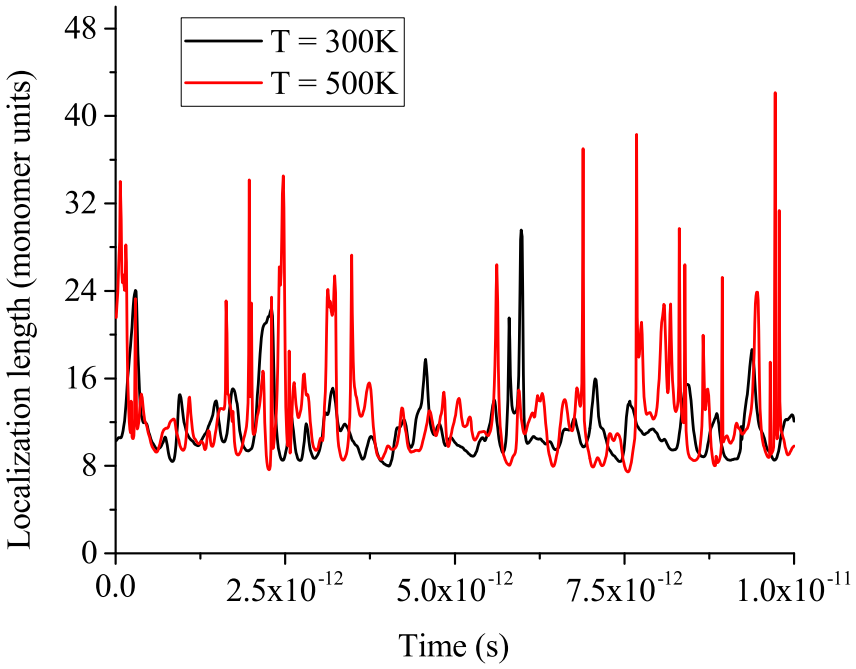

FIG. 9: The exciton localization length, given by Eq. (17), as a function of time for a single example trajectory at two high temperatures. The localization length varies significantly, with the maximum localization length being significantly larger than the localization length of the exciton-polaron, suggesting that the exciton has been excited out of the polaron potential well and into a LEGS or QEES.

B. High Temperature Exciton Dynamics

At higher temperatures, we still expect the adiabatic 'crawling' migration of the exciton-polaron, as described above, to occur. However, a second non-adiabatic mechanism for the dynamics is expected to play an important role. This mechanism involves the exciton-polaron being excited to a high enough energy by the thermal fluctuations to be excited out of the polaron potential well, resulting in a breakdown of the polaron and the exciton to enter an untrapped local exciton ground state (LEGS), or a higher energy quasi-extended exciton state (QEES). Once in this more delocalized state the exciton has quasi-band characteristics and travels quasi-ballistically.

After a relatively short period of time, however, the exciton will shed some of its excess energy and relax back into an exciton-polaron. As a result, the time-averaged exciton

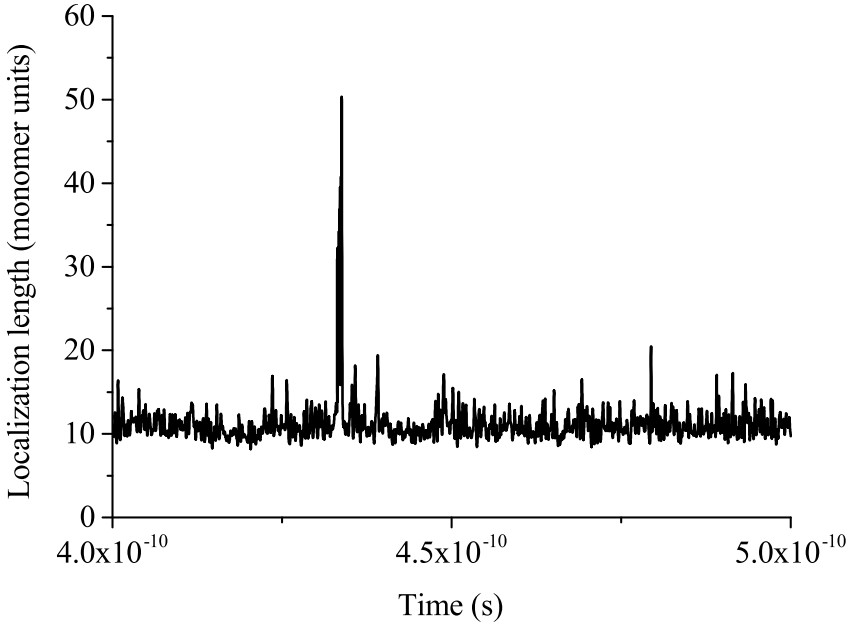

FIG. 10: The exciton localization length as a function of time for a single trajectory at 100 K. The localization length shows a sharp increase in size as the exciton is excited from an exciton-polaron state into a quasi-extended exciton state (QEES).

localization length calculations of Fig. 4 show only a slight increase in localization length with increasing temperatures, as the majority of its lifetime is still spent in self-localized exciton-polarons. The exciton localization length as a function of time for a single trajectory at two high temperatures is shown in Fig. 9. It shows that the exciton relatively frequently becomes excited into a higher lying, more spatially delocalized state, but relatively rapidly relaxes into a more localized state (either a LEGS or an exciton-polaron).

Although the exciton only spends a relatively small amount of time in these spatially extended states, it travels significantly faster while it is in them, before the wavefunction collapses randomly into a self-localized exciton-polaron. At 100 K these events are rare, allowing a single event to be investigated. Figure 10 shows how the exciton localization length varies for a single trajectory at 100 K. There is an obvious spike in the localization length, signalling that the exciton has been excited out of the self-localized exciton-polaron state and into a higher energy more delocalized state. A commensurate drop in the signed value parameter of Eq. (8) shows that the exciton has in fact been promoted into a higher

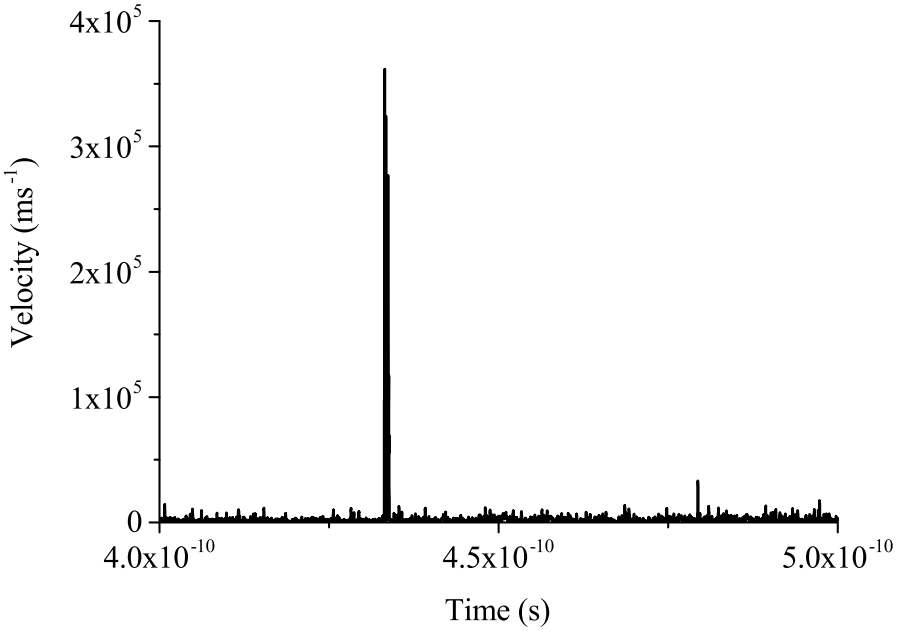

FIG. 11: The velocity of the exciton center-of-mass as a function of time for the same trajectory as Fig. 10. The large increase in the exciton localization length occurs at the same time as a large peak in the exciton velocity, indicating temporary quasi-band, quasi-ballistic transport.

energy QEES. Figure 11 shows how the velocity of the exciton state has a peak at the same point, indicating quasi-band, quasi-ballistic transport while the exciton occupies these states.

The requirement that the exciton is excited out of the polaron potential well means that this process is activated. Thus, from a simple Fermi golden rule analysis, the probability per unit time that the exciton is excited out of the polaron into a more extended state is,

$$P \sim \langle \delta\theta^2 \rangle \times \exp\left(-\frac{\Delta E}{k_B T} \right) \times \frac{1}{\ell_i \ell_f}, \tag{21}$$

where $\langle \delta\theta^2 \rangle$ is the amplitude of the torsional autocorrelation function promoting the transition, ΔE is approximately the polaron binding energy, and $1/\ell_i\ell_f$ is the squared overlap between the initial and final exciton wavefunctions. In a time t the exciton performs $M = P \times t$ hops, each of size $\sim \ell_f$. As these hops are random, the exciton executes a random walk with each hop being over a distance $\sim \ell_f$. Thus, in a time t the exciton travels a mean square distance,

$$\langle L^2 \rangle \approx \langle L_l^2 \rangle + \langle L_h^2 \rangle \tag{22}$$

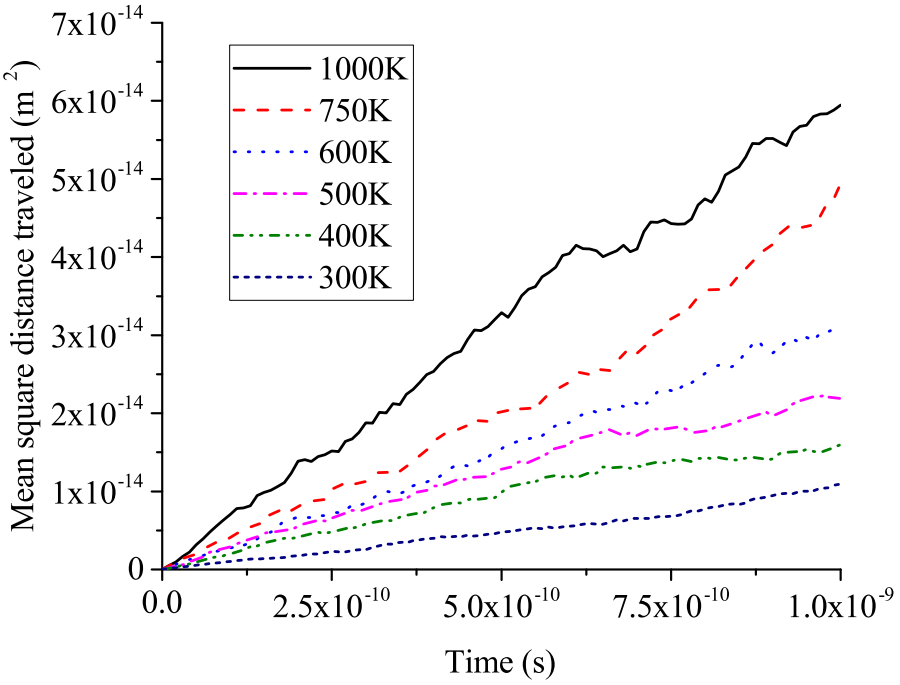

FIG. 12: The mean-square-distance traveled by an exciton at high temperatures. The motion is diffusive, as shown by the mean-square-distance, $\langle L^2 \rangle$, increasing linearly with time. Each line is an average of 150 trajectories, and $\gamma = 10^{12}$ s^{-1} throughout.

where the low temperature component of the mean square distance, $\langle L_l^2 \rangle$, is assumed to behave as an extrapolation of the low temperature results, and the high temperature component

$$\langle L_h^2 \rangle = M\ell_f^2 \sim \langle \delta\theta^2 \rangle \times \exp\left(-\frac{\Delta E}{k_B T} \right) \times \frac{\ell_f}{\ell_i} \times t. \tag{23}$$

This diffusive behavior is illustrated in Fig. 12, showing that $\langle L^2 \rangle$ increases linearly with time.

Equating $\langle L_h^2 \rangle$ with $2D_h t$ therefore implies that

$$D_h(T) \sim \langle \delta\theta^2 \rangle \times \exp\left(-\frac{\Delta E}{k_B T} \right) \times \frac{\ell_f}{\ell_i}. \tag{24}$$

From Eq. (15), $\langle \delta\theta^2 \rangle \sim T$. The initial exciton-polaron localization length, ℓ_i, is virtually independent of temperature, whereas the localization length of the LEGS or QEES, ℓ_f,

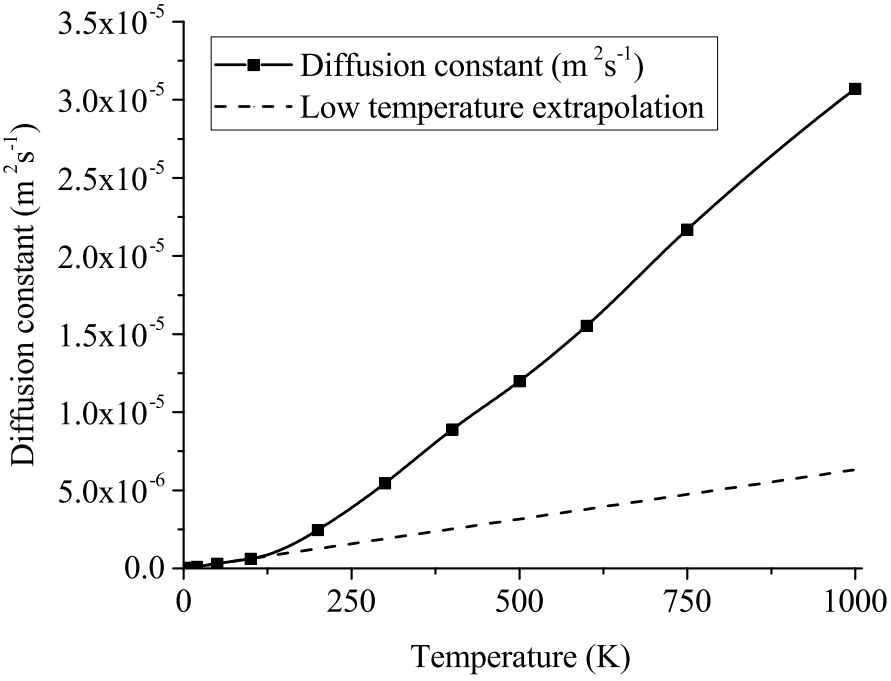

FIG. 13: The variation of the diffusion constant, D, of Eq. (19) as a function of temperature. In the high temperature regime, D still increases with increasing T. However, the gradient is significantly higher than in the low temperature regime, indicating an alternative mechanism for exciton motion begins to dominate at high temperatures.

satifies $\ell \sim \sigma^{-2/3} \sim T^{-1/3}$ (as shown in Fig. 4). Thus,

$$D_h(T) \sim T^{2/3} \exp\left(-\frac{\Delta E}{k_B T}\right), \tag{25}$$

as confirmed by Fig. 13 and Fig. 14. The agreement of the data to Eq. (25) confirms our hypothesis that the non-adiabatic exciton dynamics is an activated process via QEESs. This is reminiscent of charge transport in disordered semiconductors[30].

C. Time Dependent Schrödinger Equation Simulations

In this section we compare our simulations using the TISE with those using the TDSE. As already indicated in Section II C, the TDSE simulation fails for non-adiabatic dynamics. In the TDSE simulation the exciton wavefunction is propagated by using an 8th order Runge-Kutta numerical integrator. The TDSE method is computationally more expensive, so the

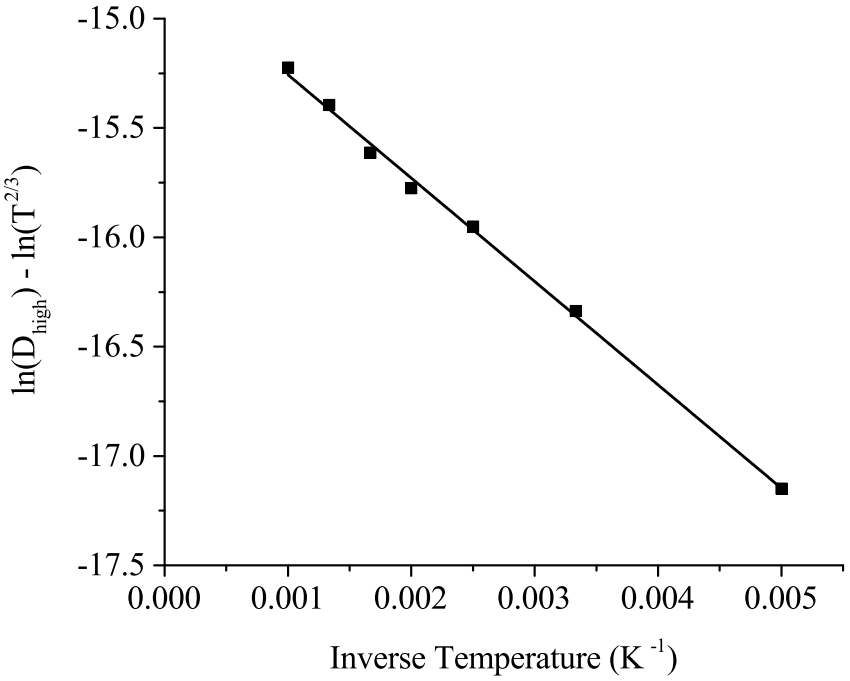

FIG. 14: The high temperature component of the diffusion constant from Fig. 13, D_{high}, is expected to show behaviour in accord with Eq. (25). As such, we expect a plot of $\ln(D_h) - \ln(T^{2/3})$ vs T^{-1} to show a linear relationship.

exciton motion was only calculated for 1 ps. When the exciton motion is adiabatic this method is in good agreement with the TISE method, as illustrated by Fig. 15. This figure shows a plot of the mean square distance traveled by the exciton as a function of time for an ensemble average of 150 simulations, and it shows that the two methods of calculation predict almost identical statistical behavior, as long as there are no non-adiabatic transitions.

The TDSE method also exhibits non-adiabatic transitions at higher temperatures, as evidenced by the overlap of the time-evolving wavefunction onto high-lying delocalized instantaneous eigenstates. This illustrates the thermal activation of a bound exciton-polaron to a quasi-band QEES. However, the subsequent evolution of the wavefunction is unphysical, as a consequence of the well-known short-comings of Ehrenfest dynamics[19]. Once the exciton has been thermally excited, we observe that the exciton remains unbound and never relaxes into a self-localized exciton-polaron. We attribute this to the neglect of correlations between the classical and quantum degrees of freedom, thus inhibiting relaxation processes.

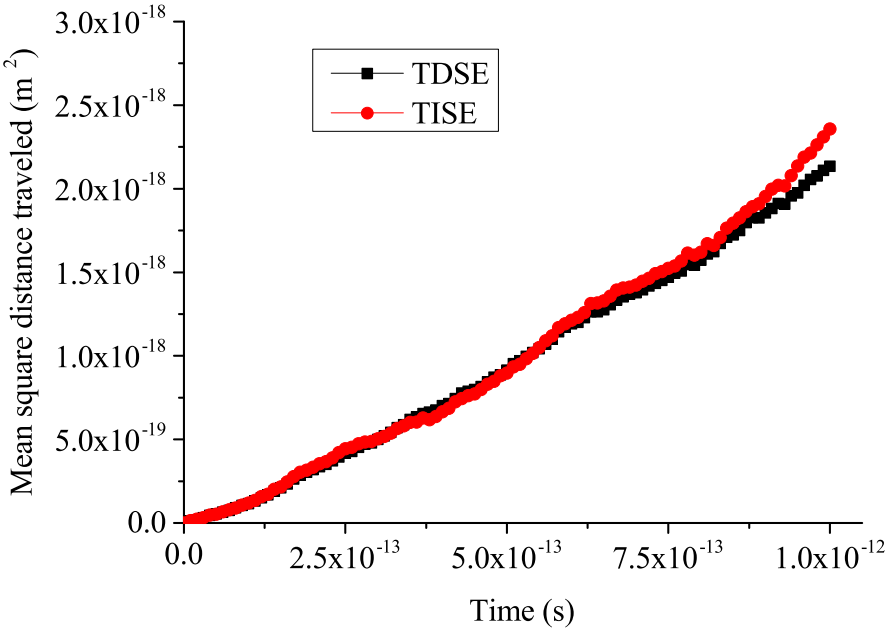

FIG. 15: The mean square distance traveled by an exciton, as calculated by the TISE simulation (red circles) and by a TDSE calculation (black squares). The simulations show an almost identical diffusion constant. The temperature of the simulations is 100 K, and $\gamma = 10^{12}$ s^{-1}.

V. CONCLUDING REMARKS

We have investigated exciton dynamics on a polymer chain in solution induced by the Brownian rotational motion of the monomers. We chose poly(para-phenylene) as a model system and modeled excitons via the Frenkel exciton Hamiltonian. The Brownian fluctuations of the torsional modes were modeled via the Langevin equation.

The rotation of monomers in polymer chains in solution has a number of important consequences for the excited state properties. First, the dihedral angles assume a thermal equilibrium which causes off-diagonal disorder in the Frenkel Hamiltonian. As has been reported before, this disorder Anderson localizes the Frenkel exciton center-of-mass wavefunctions into super-localized local exciton ground states (or LEGSs) and higher-energy more delocalized quasi extended exciton states (QEESs). LEGSs correspond to chromophores on polymer chains. The second consequence of rotations – that are low-frequency – is that their coupling to the exciton wavefunction causes local planarization and the formation of an exciton-polaron. Thus, this torsional relaxation causes additional self-localization. Finally,

and crucially, the torsional dynamics cause the Frenkel Hamiltonian to be time-dependent, leading to exciton dynamics. We identify two distinct types of dynamics.

At low temperatures the torsional fluctuations act as a perturbation on the polaronic nature of the exciton state. Thus, the dominating dynamics for the exciton at low temperatures is a small-displacement diffusive adiabatic motion of the exciton-polaron as a whole. We characterize this as 'crawling' motion along the chain. The temperature dependence of the diffusion constant has been calculated, showing that at low temperatures there is linear dependence, indicating an activationless process.

As the temperature increases, however, the diffusion constant increases at a faster than linear rate, indicating a second non-adiabatic dynamics mechanism is beginning to dominate. Although we still expect the exciton-polaron to migrate as a whole, and it is indeed observed that the exciton-polaron spends a majority of the time migrating as a single unit even at high temperatures, the exciton is also observed to be excited into higher energy more delocalized exciton states (i.e., LEGSs and QEESs) as the temperature is increased above $\approx$ 200 K. These states are not self-localized by the local torsional planarization. During the exciton's temporary occupation of a LEGS – and particularly a quasi-band QEES – its motion is semi-ballistic with a potentially large group velocity. After a short period of rapid transport, the exciton wavefunction collapes again into an exciton-polaron state. We characterize this as intra-band 'hopping' motion along the chain and provide a semi-quantitative theory for this process in agreement with the data.

Overall, the exciton is calculated to migrate a significant distance along the polymer chain before it radiatively decays. For example at room temperature, it would be expected to move a distance of $\sim$ 100 nm. These distances are significantly larger than distances previously observed for exciton migration in solid state polymer aggregates[31–33], which can be attributed to the fact that the migration distances here are contour lengths rather than real space, and they would be far smaller in a coiled polymer chain. In addition, in the solid state the torsional motion will be impeded, meaning that migration distances are likely to be significantly shorter, with resonant exciton transfer between nearby chromophores playing a greater role.[22]

Acknowledgments W.B. thanks D. Yaron for useful discussions.

Corresponding authors Email addresses: oliver.tozer@chem.ox.ac.uk and william.barford@chem.ox.ac.uk

---

[1] D. V. Makhov and W. Barford, *Phys. Rev. B*, **81**, 165201 (2010)

[2] P. W. Anderson, *Phys. Rev.*, **109**, 1492 (1958)

[3] P. Prins, F. C. Grozema, and L. D. A. Siebbeles, *J. Phys. Chem. B*, **110**, 14659 (2006)

[4] M. Hultell and S. Stafström, *Phys. Rev. B*, **79**, 014302 (2009)

[5] M. Jakobsson, M. Linares and S. Stafström, *J. Chem. Phys.*, **137**, 114901 (2012)

[6] N. M. Albu and D. J. Yaron, *J. Chem. Phys.*, **138**, 224902 (2013)

[7] R. P. Fornari and A. Troisi, *Phys. Chem. Chem. Phys.*, **16**, 9997 (2014)

[8] M. Bednarz, V. A. Malyshev and J. Knoester, *J. Chem. Phys.*, **120**, 3827 (2004)

[9] N. M. Albu and D. J. Yaron, *J. Phys. Chem. C*, **117**, 12299 (2013)

[10] P. Langevin, *C. R. Acad. Sci. (Paris)*, **146**, 530 (1908)

[11] W. F. van Gunsteren and H. J. C. Berendsen, *Molecular Physics*, **45**, 637 (1982)

[12] M. P. Allen, *Molecular Physics*, **40**, 1073 (1980); *Molecular Physics*, **47**, 599 (1982)

[13] R. Kubo, *Rep. Prog. Phys.*, **29**, 255 (1966)

[14] A. V. Malyshev and V. A. Malyshev, *Journal of Luminescence*, **94-95**, 369 (2001)

[15] W. Barford and D. Trembath, *Phys. Rev. B*, **80**, 165418 (2009)

[16] O. R. Tozer and W. Barford, *Phys. Rev. B*, **89**, 155434 (2014)

[17] P. Rebentrost, M. Mohseni, I. Kassai, S. Lloyd, and A. Aspuru-Guzik, *New Journal of Physics*, **11**, 033003 (2009)

[18] J. Frenkel, *Phys. Rev.*, **37**, 1276 (1931)

[19] A. P. Horsfield, D. R. Bowler, A. J. Fisher, T. N. Todorov, and C. G. Sánchez, *J. Phys.: Condens. Matter*, **16**, 8251 (2004)

[20] O. R. Tozer and W. Barford, *J. Phys. Chem. A*, **116**, 10310 (2012)

[21] Although considering all dipole-dipole interactions moves the band edge[8] from $-2J$ to $-2.4J$, these longer range interactions are disregarded in this work. In addition to the simplicity this provides our model, the justification for this approximation is that these longer range dipole-dipole interactions, which decay as r_{ij}^{-3}, can be considered to be perturbations on the zeroth-order Hamiltonian (i.e., that containing nearest neighbour interactions only) that cause exciton

diffusion between the zeroth-order eigenstates by non-adiabatic processes (i.e., Förster resonant exciton transfer). Although this mechanism is significant for exciton migration between polymer chains in the solid state, it has a much smaller effect on intrachain exciton diffusion[22].

[22] W. Barford, E. R. Bittner and A. Ward *J. Phys. Chem. A*, **116**, 10319 (2012); W. Barford and O. R. Tozer, *J. Chem. Phys.*, **141**, 164103 (2014)

[23] L. D. Landau, *Z. Phys.*, **3**, 664 (1933)

[24] The terms 'self-localization' and 'self-trapping' should not be confused. Here we follow the customary literature definition where 'self-trapping' means a particle associated with nuclear displacements, which together are delocalized in space. 'Self-localization' (or 'auto-localization'[23]), on the other hand, refers to a polaron in the classical, adiabatic limit which is localized in space as a consequence of both disorder (which breaks translational symmetry) and of the polaron's diverging effective mass.[16]

[25] M. Capone, W. Stephan, and M. Grilli, *Phys. Rev. B*, **56**, 4484 (1997)

[26] F. C. Spano and H. Yamagata, *J. Phys. Chem. B*, **115**, 5133 (2010)

[27] W. Barford and M. Marcus, *J. Chem. Phys.*, **141**, 164101 (2014); M. Marcus, O. R. Tozer and W. Barford *J. Chem. Phys.*, **141**, 164102 (2014)

[28] A. Ruseckas, P. Wood, I. D. W. Samuel, G. R. Webster, W. J. Mitchell, P. L. Burn and V. Sundström *Phys. Rev. B*, **72**, 5 (2005)

[29] W. Barford, I. Boczarow and T. Wharram *J. Phys. Chem. A*, **115**, 9111 (2011)

[30] N. F. Mott and E. A. Davis, *Electronic Processes in Non-crystalline Materials*, Oxford University Press, Oxford (1979)

[31] S. R. Scully and M. D. McGhee, *J. Appl. Phys*, **100**, 034907 (2006)

[32] A. J. Lewis, A. Ruseckas, O. P. M. Gaudin, G. R. Webster, P. L. Burns and I. D. W. Samuel, *Org. Electron.*, **7**, 452 (2006)

[33] D. E. Markov, E. Amsterdam, P. W. M. Blom, A. B. Sieval and J. C. Hummelen, *J. Phys. Chem. A*, **109**, 5266 (2005)